

# **Novel Carbon Materials from the Hydrothermal Carbonization of Biomass**

---

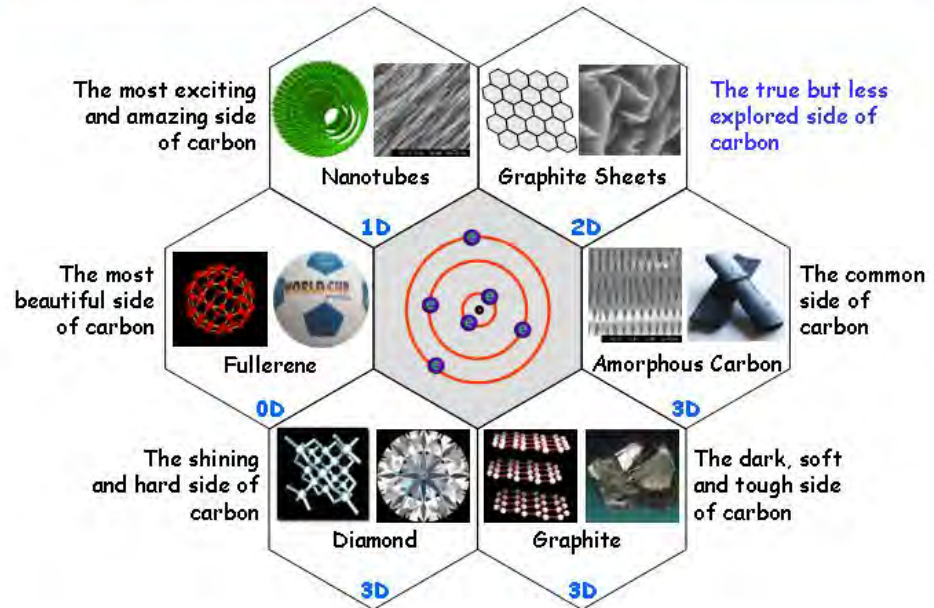
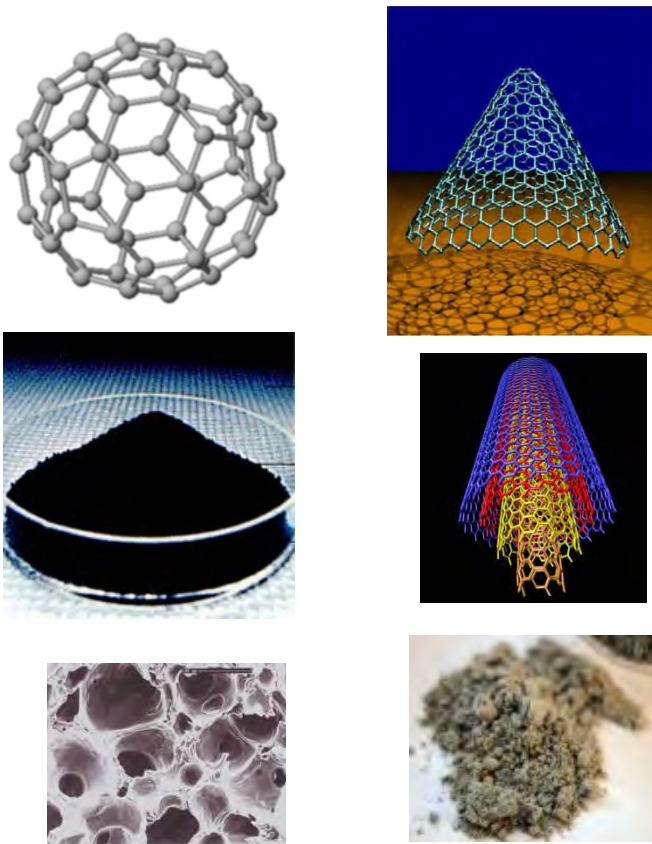
**Shouxin Liu**

***College of Material Sciences and Engineering  
Northeast Forestry University  
Harbin, 150040, China***

# 1. BACKGROUND

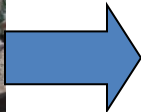
Energy shortage, environmental crisis, and developing customer demands have driven people to find facile, low-cost, environmentally friendly, and nontoxic routes to produce novel functional materials that can be commercialized in the near future.

# The carbon family



Biomass is a qualified carbon raw material for the synthesis of valuable carbon materials because it is available in high quality (e.g., as pure saccharose) and huge amount, and is an environmental friendly renewable resource.

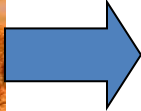
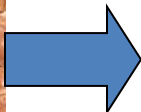
Biomass



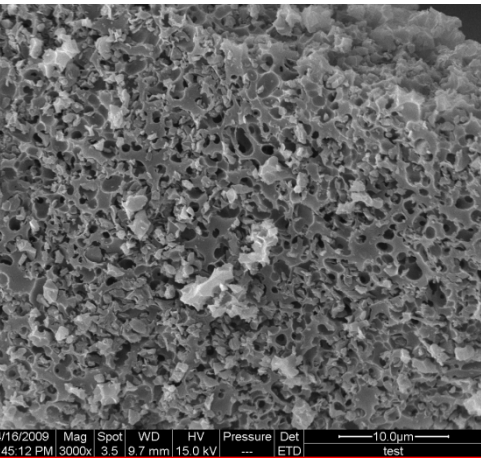
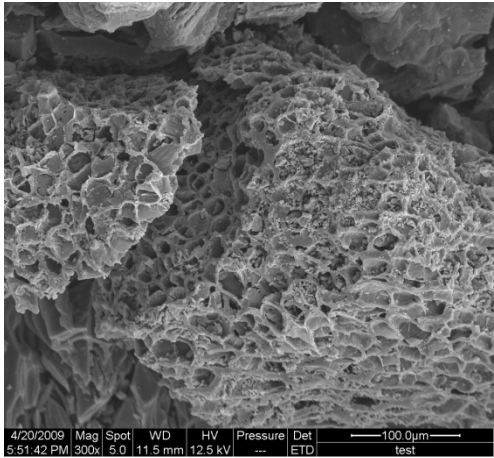
Carbon



杏核



Biomass



Carbon

● Carbon materials fabricated from waste biomass have shown promising applications as sorption materials, hydrogen storage, biochemicals, and others.

● The problem is that there is still no general and satisfactory process for the production of valuable carbon materials from crude biomass to date.



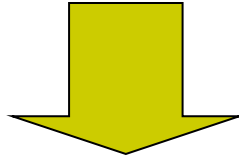
# Hydrothermal carbonization

---

**Hydrothermal carbonization (HTC) process of biomass (either of isolated carbohydrates or crude plants) is a promising candidate for the synthesis of novel carbon-based materials with a wide variety of potential applications.**

---

According to different experimental conditions and reaction mechanisms, two HTC processes can be classified.

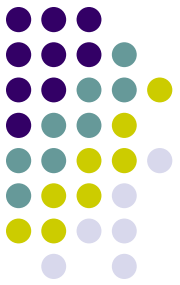


Hydrothermal Carbonization at High Temperature:  
Carbon nanotubes, graphitic carbon materials, and activated carbon materials

Hydrothermal Carbonization at Low Temperature:  
Synthesis of Highly Reactive Carbonaceous Nanostructures

Carbon-Based Nanocomposites:  
Encapsulation and In situ  
Efficient Loading with Metal Nanoparticles

The HTC process at low temperature is apt to generate monodispersed colloidal carbonaceous spheres,

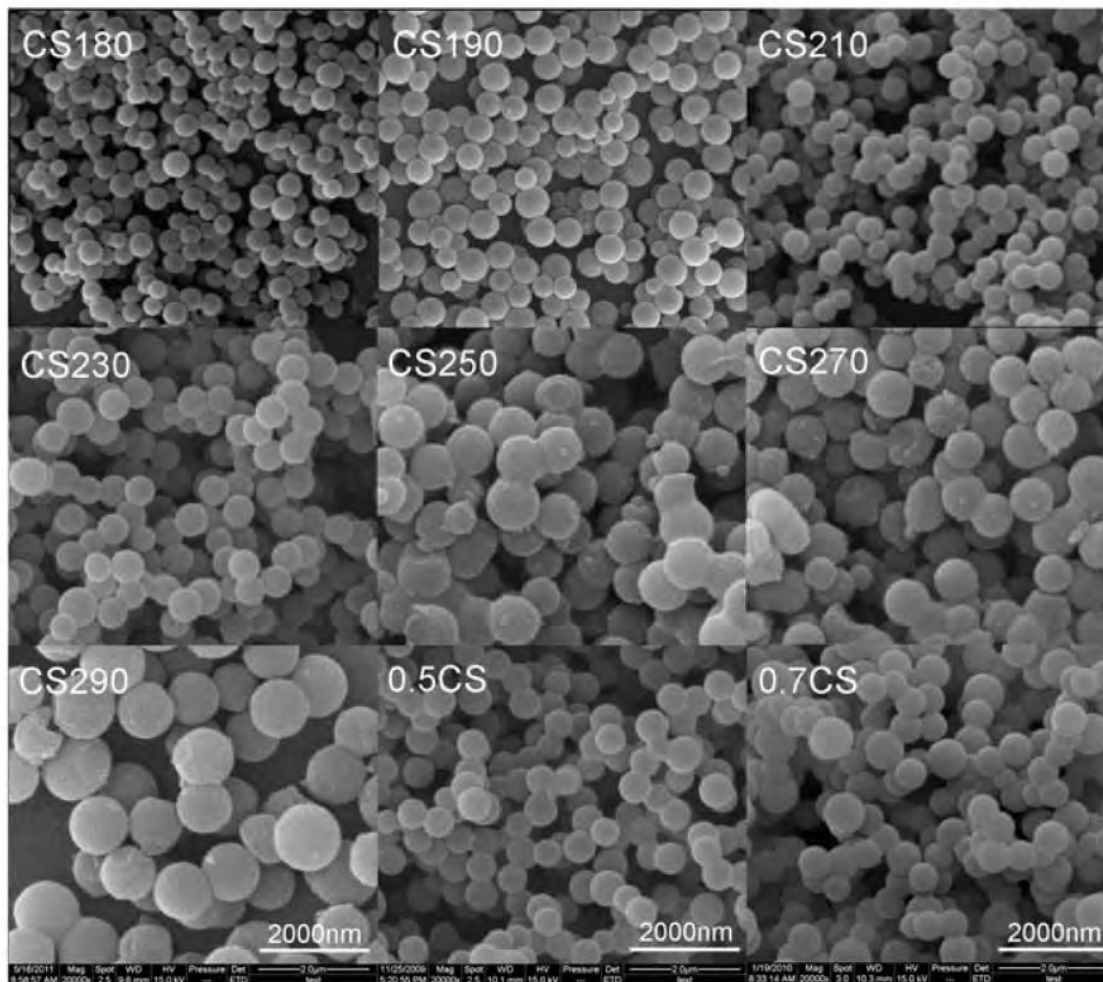


## 2. **HTC of Glucose for Carbon Sphere**

### **Control of the morphology and chemical properties of carbon spheres prepared from glucose by a hydrothermal method**

Preparation of CSs Forty milliliters of glucose solution (0.3–0.7 mol/L) was transferred into a stainless-steel autoclave with a capacity of 60 mL, sealed, and heated at 140–290 ° C for 3–7 h. When the reaction was completed, the autoclave was cooled to room temperature. The black precipitate that formed was collected and washed with water, pure ethanol, and acetone for three times.





when the temperature was increased from 180 to 290 ° C, the diameter of the CSs increased from 300 to 1200 nm

as the glucose concentration increased from 0.3 to 0.7 mol/L, the diameter of the CSs increased from 400 to 650 nm

FIG. 1. Scanning electron microscopy (SEM) images of CS180, CS190, CS210, CS230, CS270, CS290, and 0.5CS, 0.7CS.

At low temperature (230 ° C), the CSs had a smooth surface and regular shape. When T.230 ° C, the surface of the CSs became rough, and fused spheres and irregular spherical particles appeared

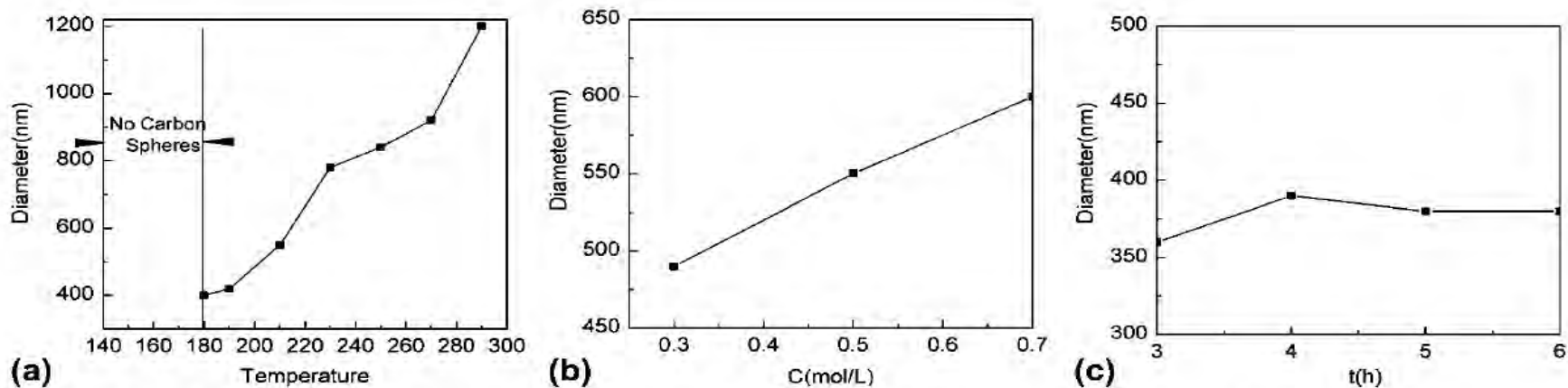


FIG. 2. Effects of (a) temperature, (b) concentration, and (c) reaction time on the size of the carbon spheres (CSs).

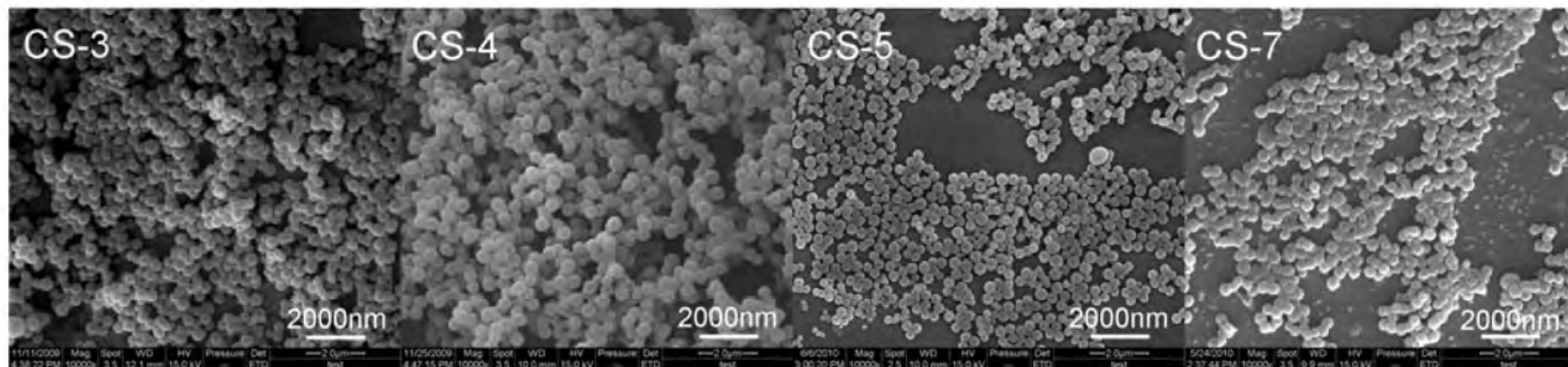


FIG. 3. SEM images of CS-3, CS-4, CS-5, and CS-7.

When the reaction time was increased from 3 to 7 h, the diameter of the CSs remained around 400 nm [Fig. 2 (c)], but the morphology changed. With a reaction time of 3 or 4 h, CSs with regular shapes and smooth surfaces were produced. When the reaction time was increased to 5 h, the spheres became irregular and some fused together. With a reaction time of 7 h, most of the CSs aggregated. This indicates that the reaction time can be used in shape control and that 3–4 h is the optimum

These changes indicate that amorphous carbon, microcrystalline carbon, and turbostratic carbon coexist in the CSs and that phase transformation from amorphous to the turbostratic stacking is induced by carbonization.

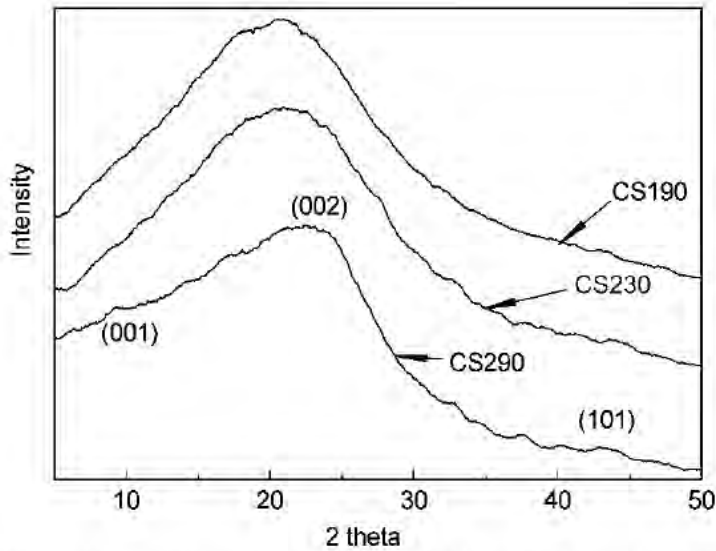
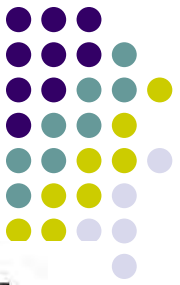


FIG. 4. X-ray diffraction patterns of CS190, CS230, and CS290.

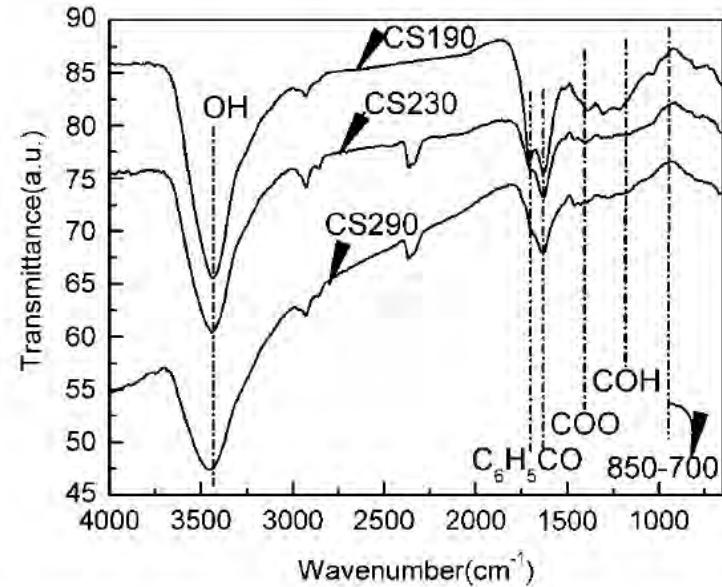


FIG. 5. Fourier-transform infrared spectra of CS190, CS230, and CS290.

These results indicate that there are many  $-OH$ ,  $C_5O$ , and  $C_6H_5-C_5O$  groups on the surface of the CSs.

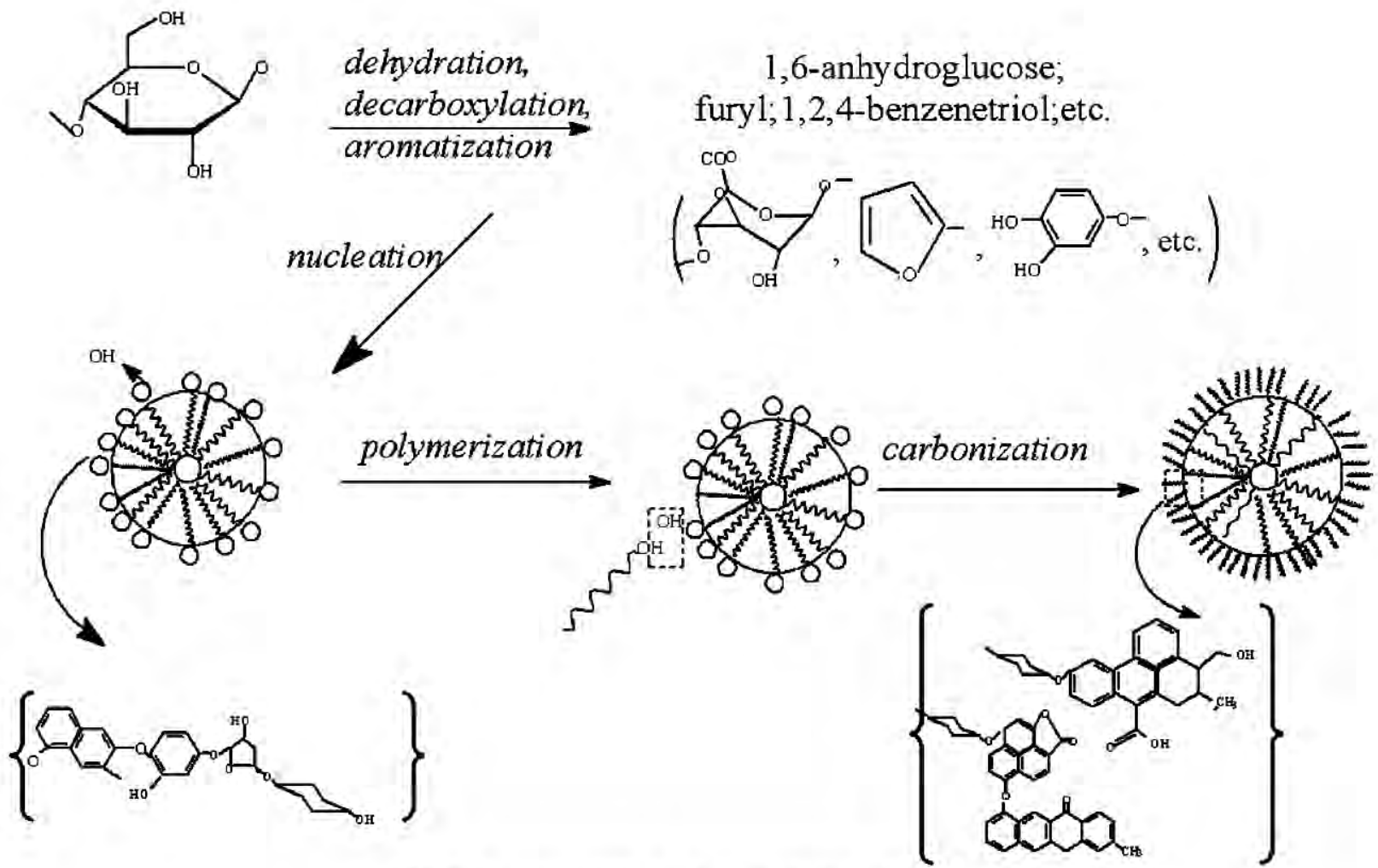


FIG. 7. Formation of CSs by glucose hydrothermal treatment.



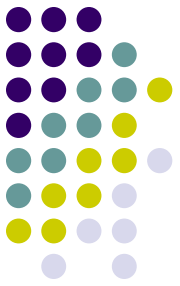
### 3.

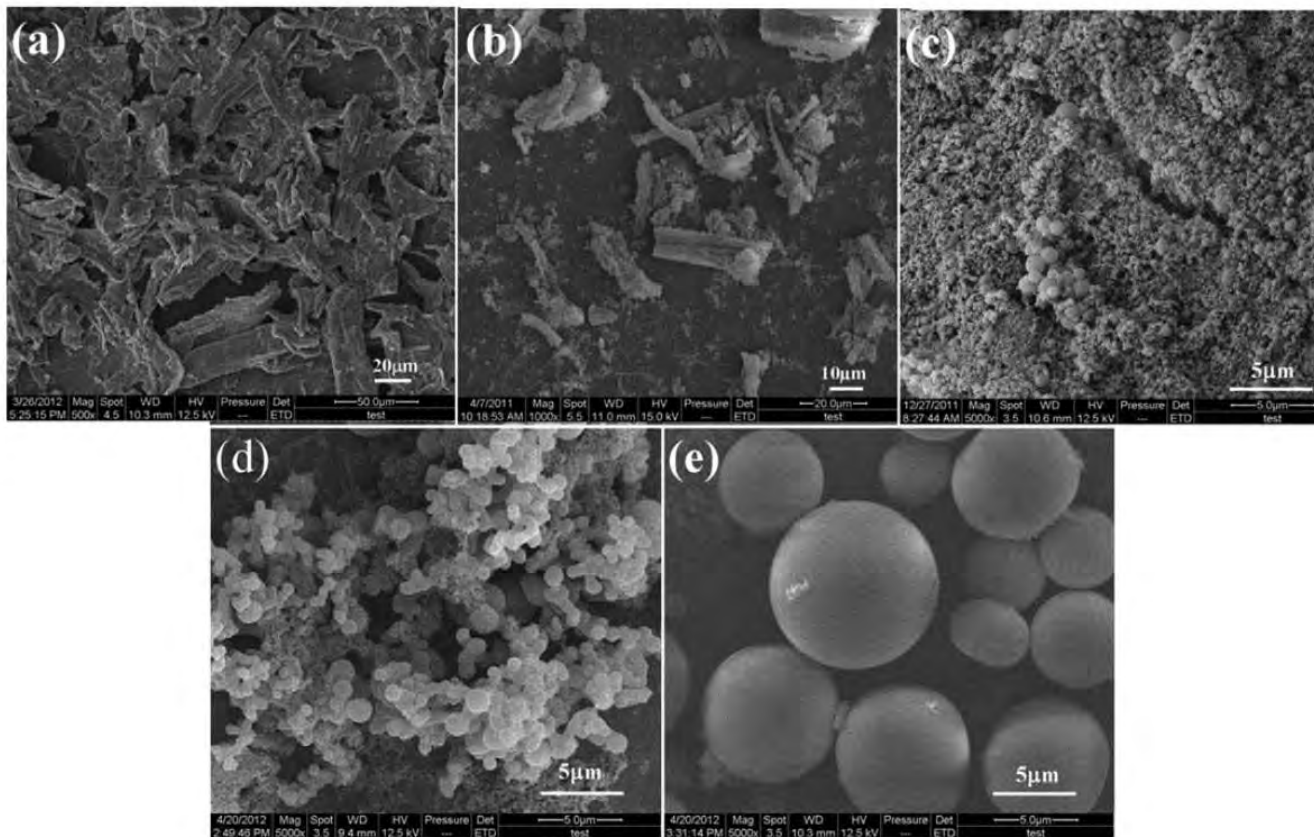
## HTC of Cellulose for Carbon Sphere

Carbon spheres obtained via citric acid catalysed hydrothermal carbonisation of cellulose

Due to the strong resistance of lignin to hydrolysis, it is hard to directly convert cellulose and lignocellulosic biomass into carbon like saccharides. It is desirable to find a catalyst which can promote efficient carbonization of cellulose via hydrolysis–dehydration.

This work focused on the fabrication of the carbon spheres with controllable sizes and oxygen containing functional groups on the surface, using a hydrothermal carbonisation method. Cellulose was used as raw material and citric acid as catalyst. Effects of the hydrothermal conditions (concentration of citric acid and reaction temperature) on size and morphology were investigated. A possible carbon sphere formation mechanism was proposed.

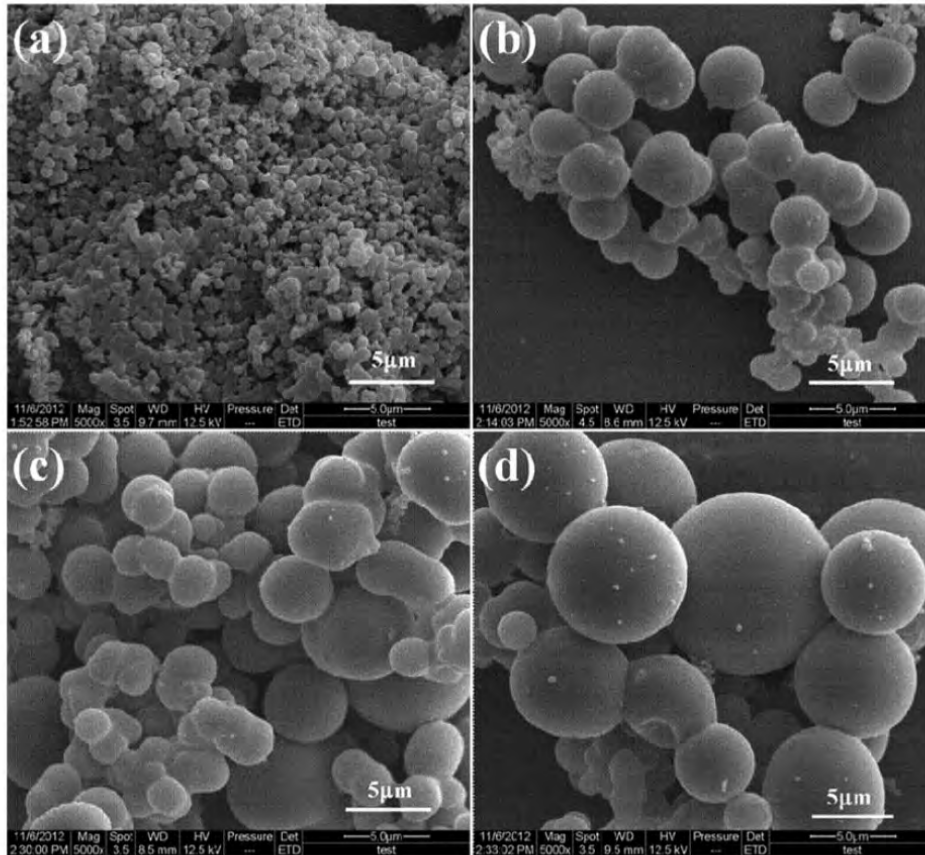
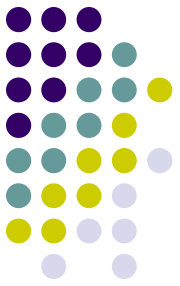




1 Images (SEM): *a* original cellulose and cellulose hydrothermally treated at *b* 190°C, *c* 200°C, *d* 220°C and *e* 240°C

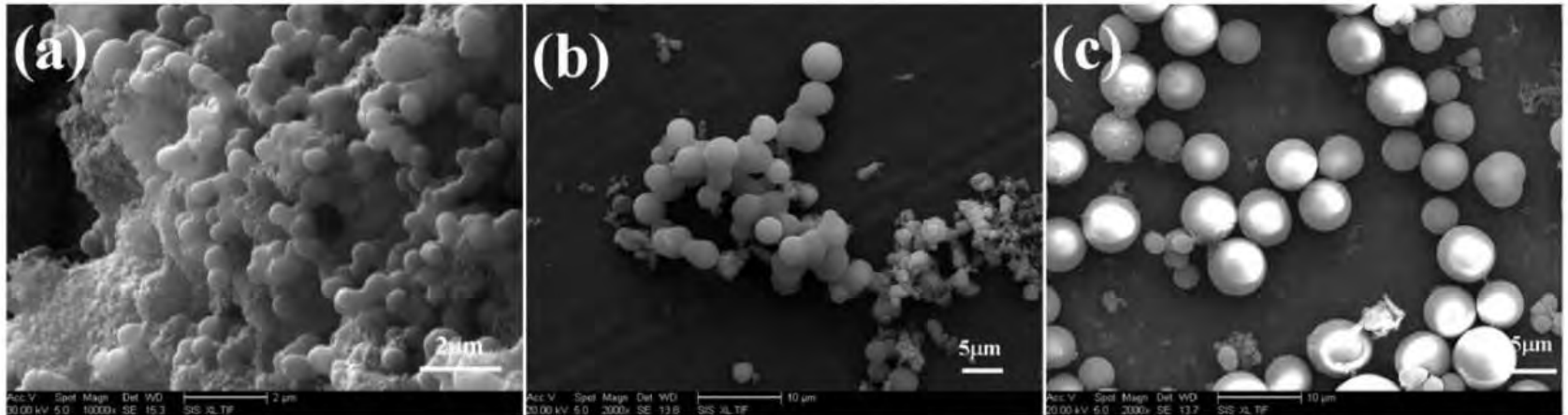
- At low temperature (190°C), the morphology of the solid product (Fig. 1b) was similar to that of original cellulose (Fig. 1a) and no spherical products were observed.
- At T=200°C, the carbon spheres of diameter 0.5–1 mm appeared.
- With further increases in the hydrothermal temperature from 200 to 240°C, the carbon spheres size increased from 0.5–1 to 5–10 mm (Fig. 1c–e), and the dispersion was improved.





2 Images (SEM) of carbon spheres hydrothermal synthesised at 240°C for *a* 6 h, *b* 8 h, *c* 10 h and *d* 12 h

with the increase of reaction time from 6 to 12 h, morphology of carbon spheres unchanged, but the diameter increased from 0.5 to 5 μm.



3 Images (FESEM) of carbon spheres prepared using *a* 1 wt-% citric acid, *b* 2 wt-% citric acid and *c* 2.5 wt-% citric acid

It is clear that citric acid can decrease aggregation of carbon particles significantly. When citric acid dosage of 2.5 wt-% was used, well dispersed carbon spheres with uniform diameter of 5  $\mu\text{m}$  can be obtained. Also, it can be seen that higher citric acid dosage was benefited for large particle formation.

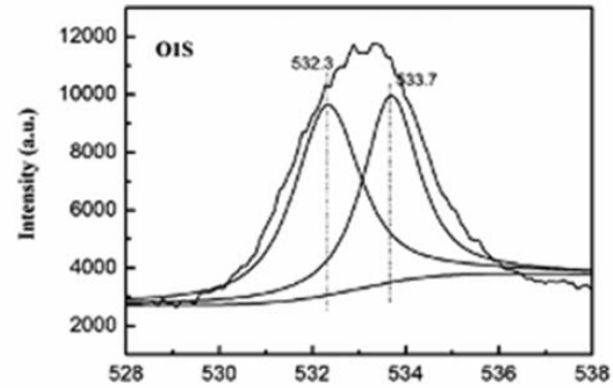
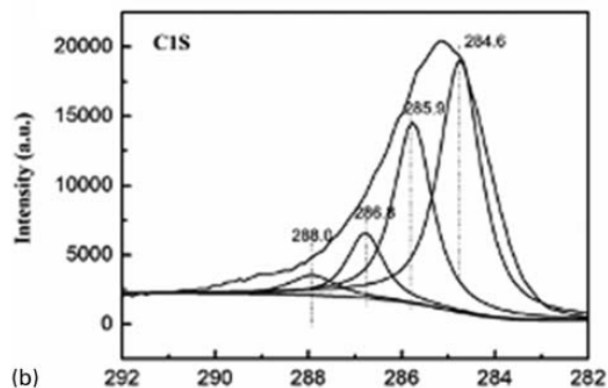
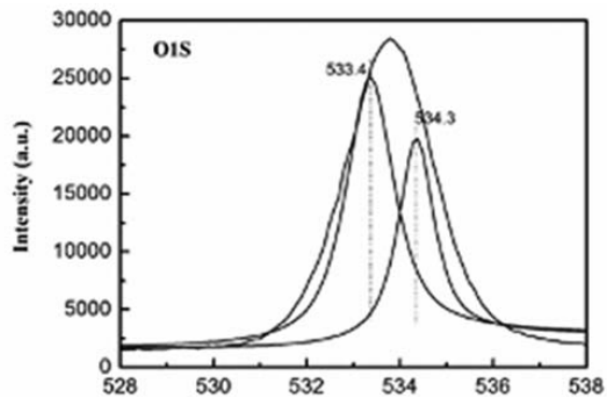
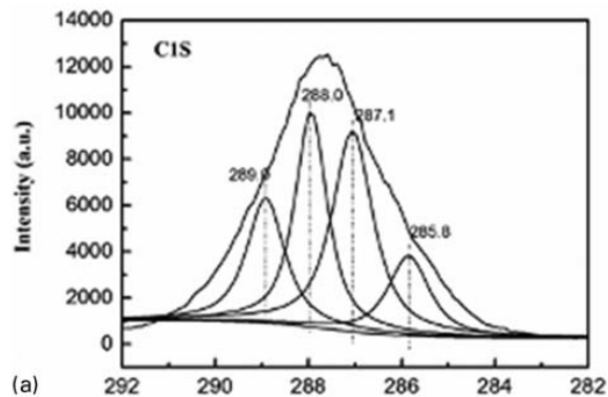


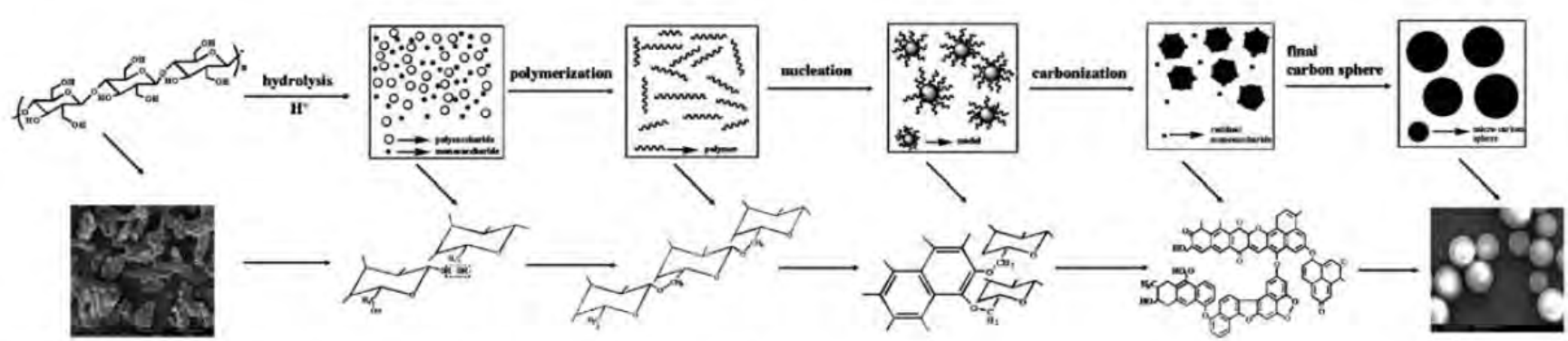
**Table 1** Chemical elemental analysis and product yields for carbon spheres obtained by hydrothermal treatment at temperatures from 190 to 240°C\*

Sample	Chemical composition/wt-%					Yield/%
	C/wt-%	H/wt-%	O/wt-%	O/C/at-%	H/C/at-%	
Original cellulose	55.00	7.1	37.9	0.689	0.129	...
CS190	56.53	7.16	36.31	0.6423	0.1267	...
CS200	78.35	5.57	16.08	0.2052	0.0711	34.2
CS220	78.67	5.46	15.87	0.2017	0.0694	38.6
CS240	79.24	5.63	15.13	0.1909	0.071	55.9

\*The carbon spheres obtained from cellulose after hydrothermal treatment for 12 h at 190, 200, 220 and 240°C were labelled CS190, CS200, CS220 and CS240 respectively.

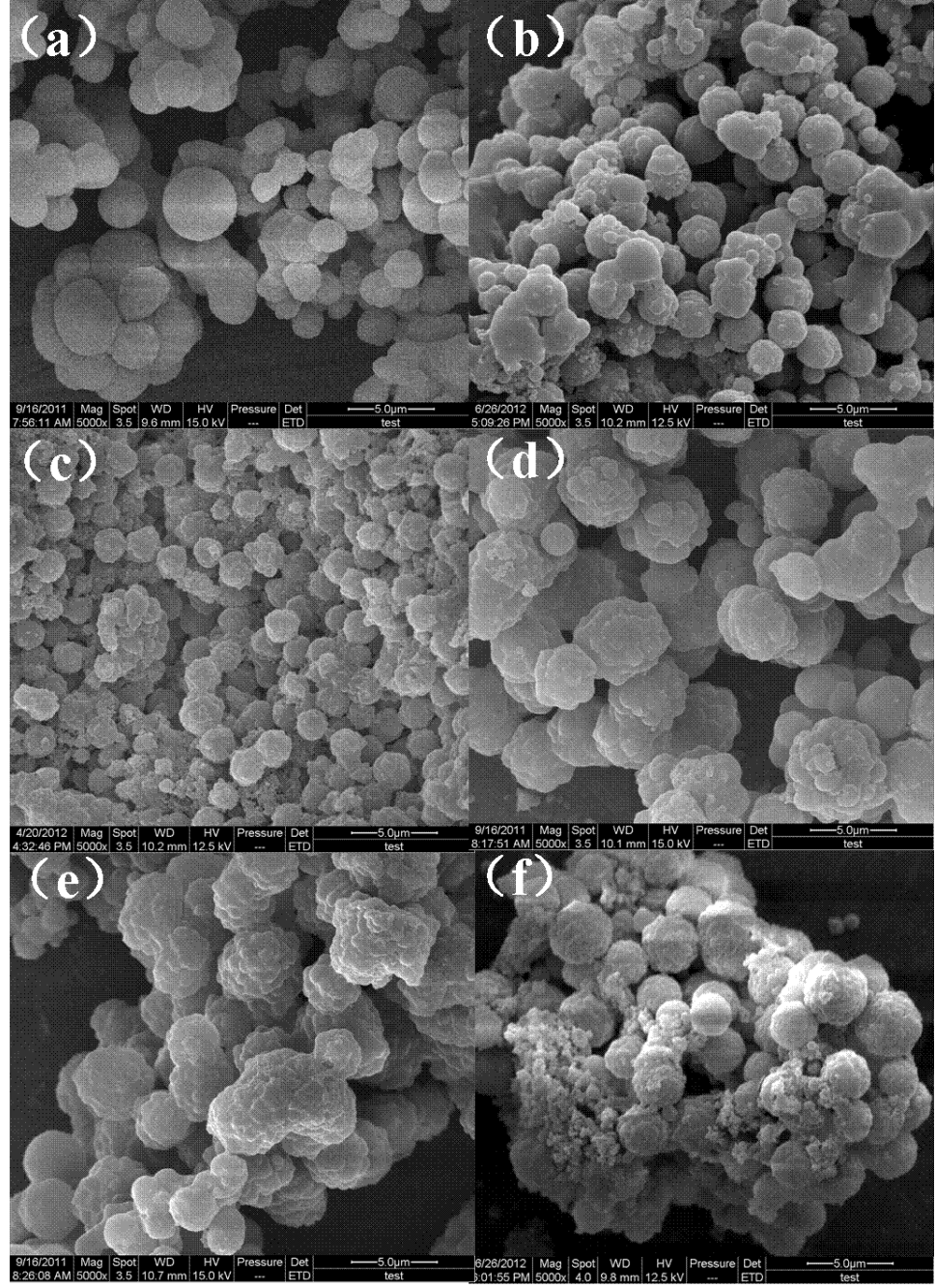
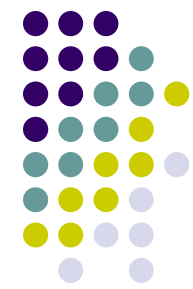


In the first step, the citric acid catalysed hydrolysis of cellulose produced oligosaccharides, monomers (glucose and fructose) and other by-products. The polysaccharides from cellulose also hydrolysed into monomers, which continued to react with the remaining H<sup>+</sup> in the solution. Then the polymerisation of monomers was built up by intermolecular dehydration, leading to the formation of soluble polymers. The concentration of these polymers was critical to the nucleation. When the concentration reached the critical supersaturation point, a short single nucleation burst occurred with the progress of dehydration and aromatization. At this stage, the initial carbon spheres with the diameters of submicrometre size were formed.



7 Formation of carbon spheres by cellulose hydrothermal treatment





Flower type carbon microspheres (CSC) were prepared from cellulose using acrylic acid as acid catalyst and self-assemble by hydrothermal treatment. The morphology and diameter size of carbon microspheres can be controlled by the reaction hour, reaction temperature, and the concentration of acrylic acid.

Fig. 4-1 SEM images of MCC treated for different temperature(a) 210°C , (b) 220 °C , (c) 230 °C (d) 240 °C (e) 250 °C (f) 260 °C

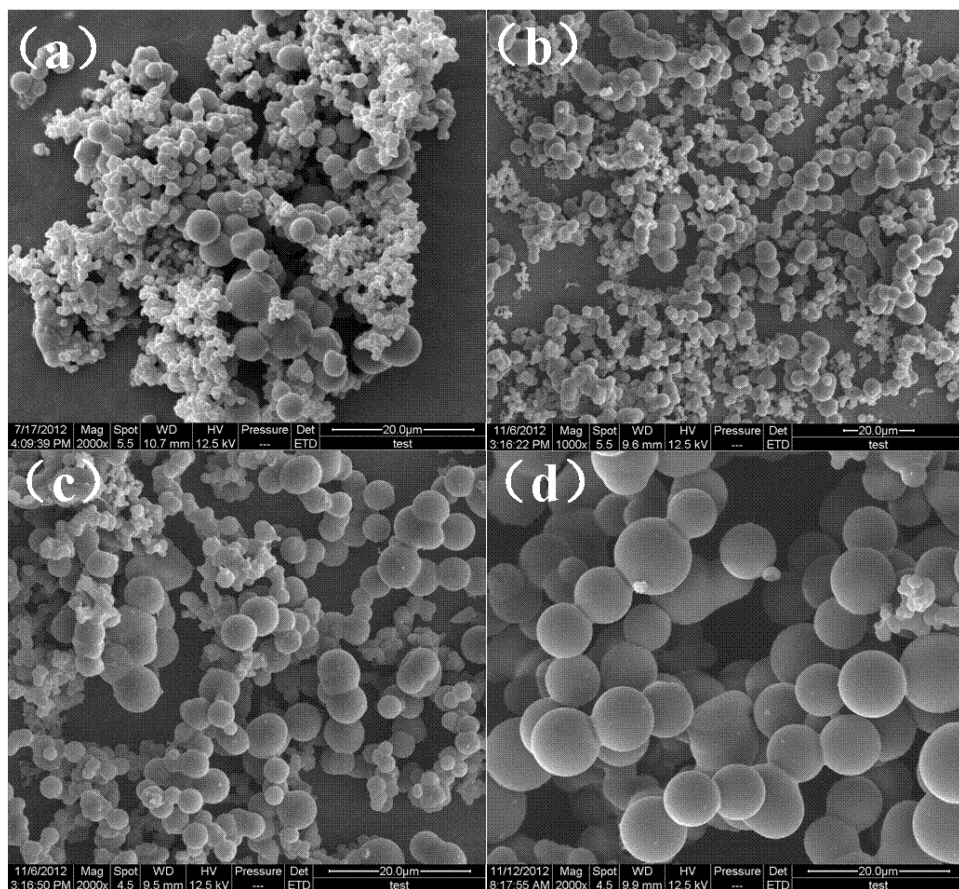
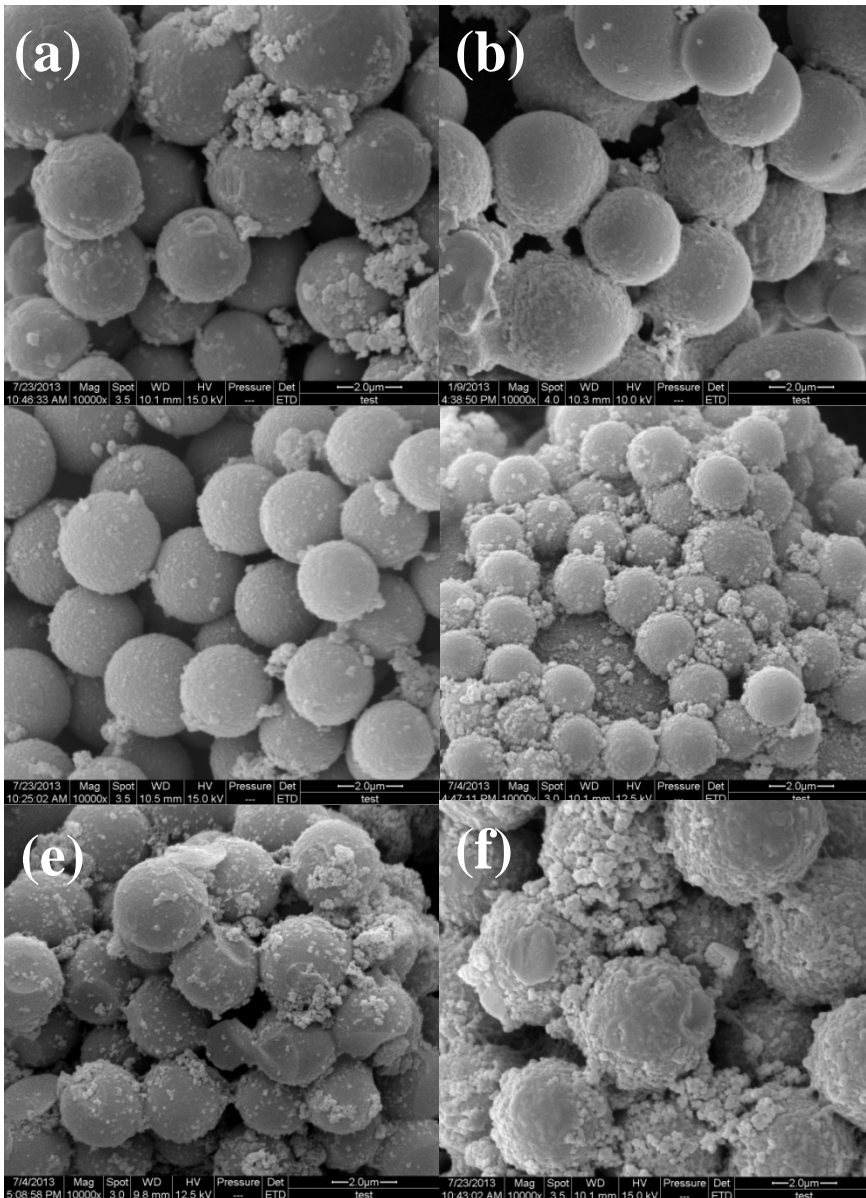
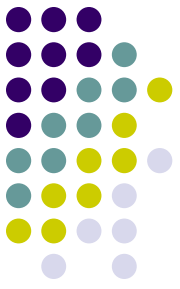


Fig. 5-1 SEM images of MCC treated using different reaction time (a) 4 h, (b) 6 h (c) 8 h (d) 10 h

Spherical carbon rich in  $-\text{SO}_3\text{H}$  was prepared from cellulose in present of concentrated sulfuric acid by hydrothermal treatment, which exhibited high catalytic activity for the hydrolysis cellulose.





Mesoporous carbon spheres (CSF) with tunable morphology and pore structure were prepared from cellulose via soft-templated and the hydrothermal method. The diameter size of carbon spheres can be controlled by the concentration of F127, the morphology and the pore structure can be tunable by carbonization temperature.

Fig. 6-2 SEM images of CSF burning at different temperature (a) 600 °C (b) 700 °C (c) 750 °C (d) 800 °C (e) 850 °C (f) 900 °C

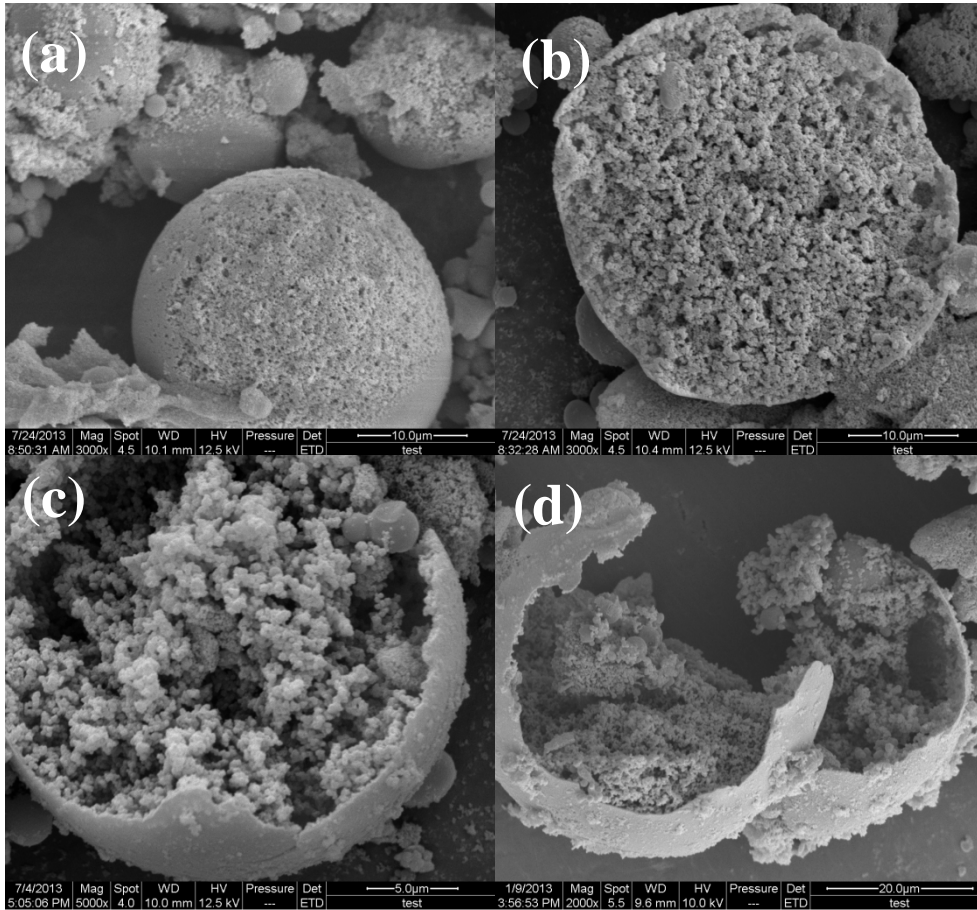
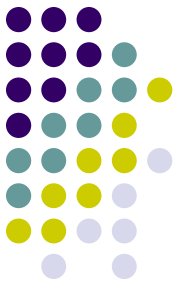


Fig. 6-5 SEM images of CSF3 burning at different temperature (a) 600 °C (b) 700 °C (c) 800 °C (d) 900 °C

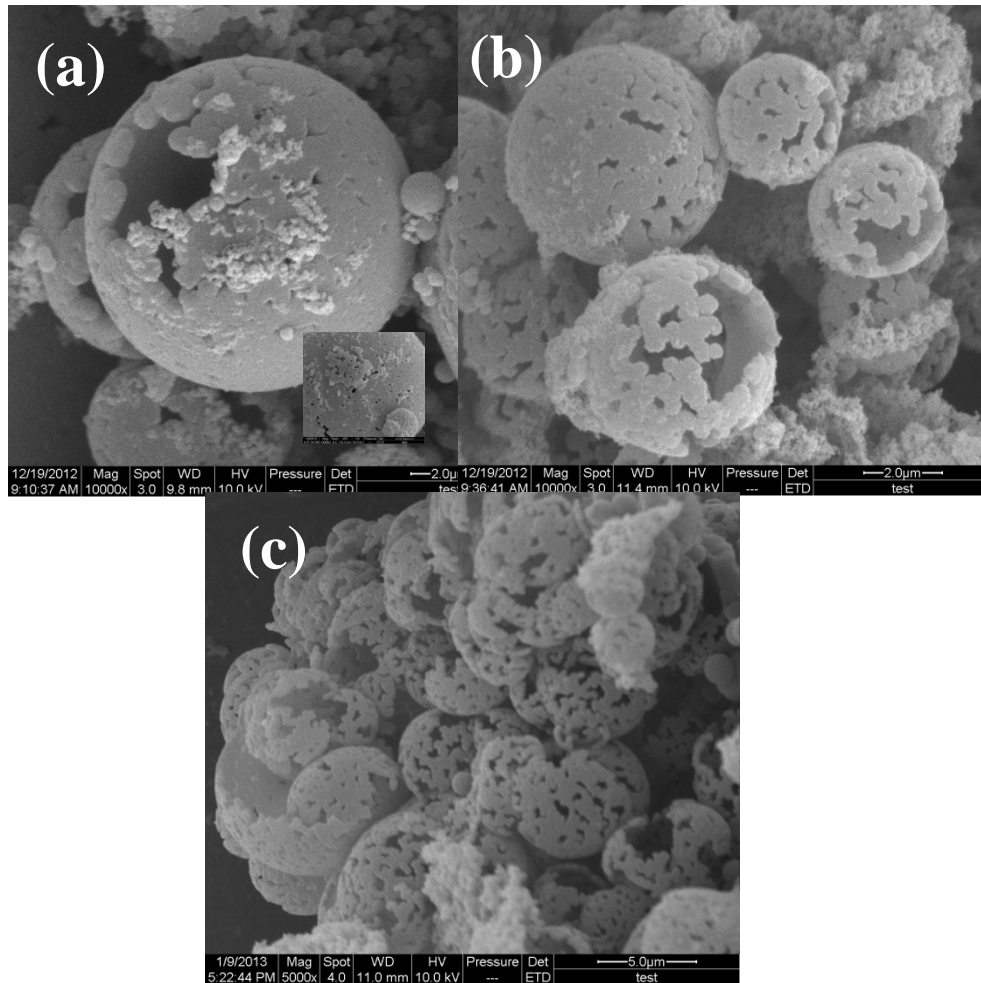
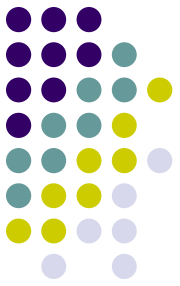


Fig. 6-8 SEM images of CSF3 burning at different temperayure (a) 700 °C (b) 800 °C (c) 900 °C



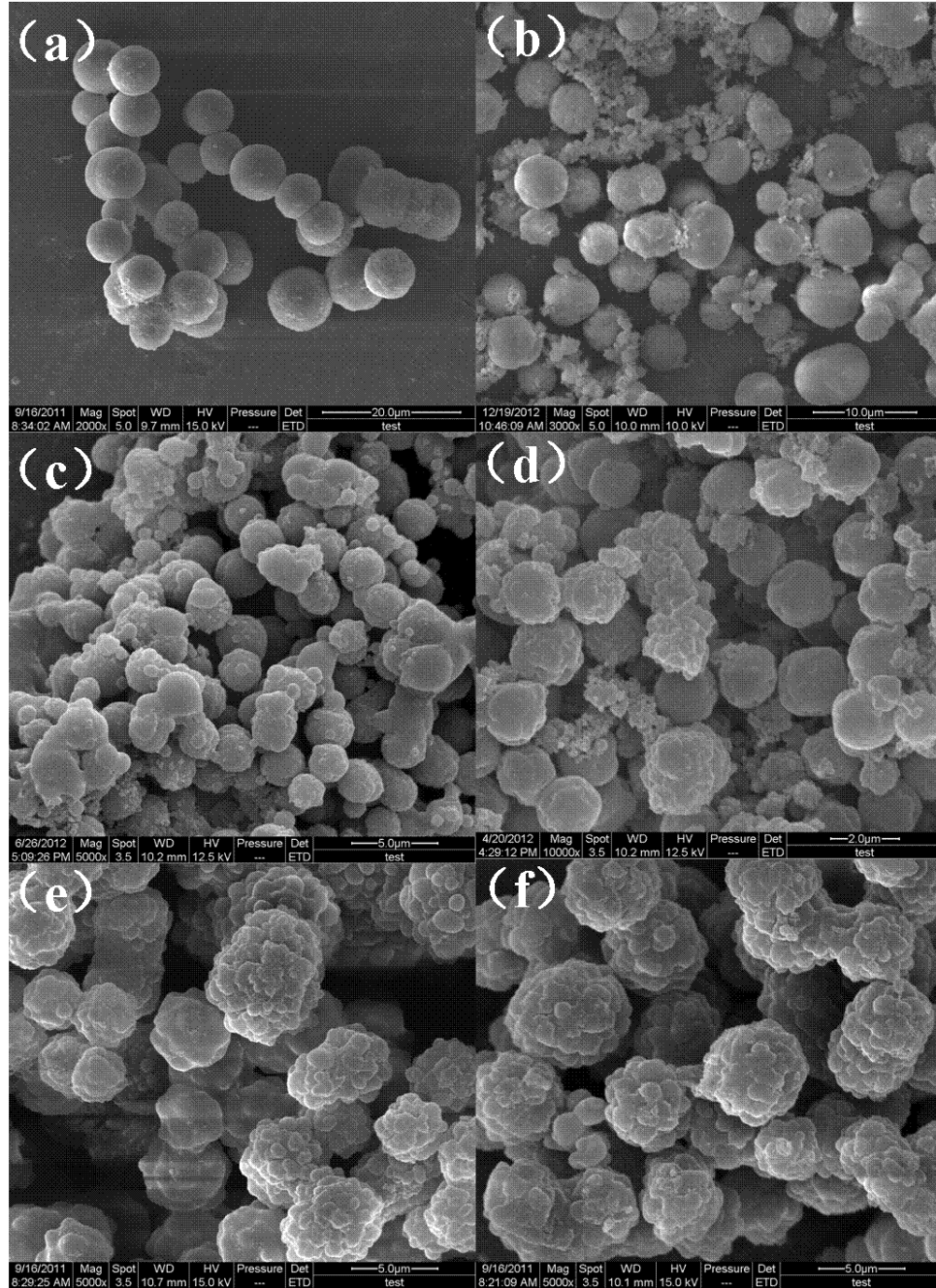
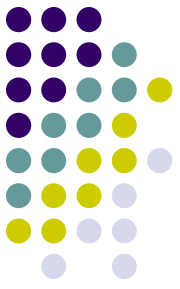


Fig. 4-3 SEM images of production treated using different concentration of acrylic acid(a)1%, (b) 2% (c) 4% (d) 6% (e) 8% and (f) 10%

# 4.

## Application of Hydrothermal Carbon Sphere

### Carbonaceous Materials as Sacrificed Template: Synthesis of $\text{TiO}_2$ hollow spheres



Because of the facile removal of the carbonaceous materials fabricated by the HTC process, the as-synthesized carbonaceous spheres have been used as sacrificed templates for fabricating hollow spheres,

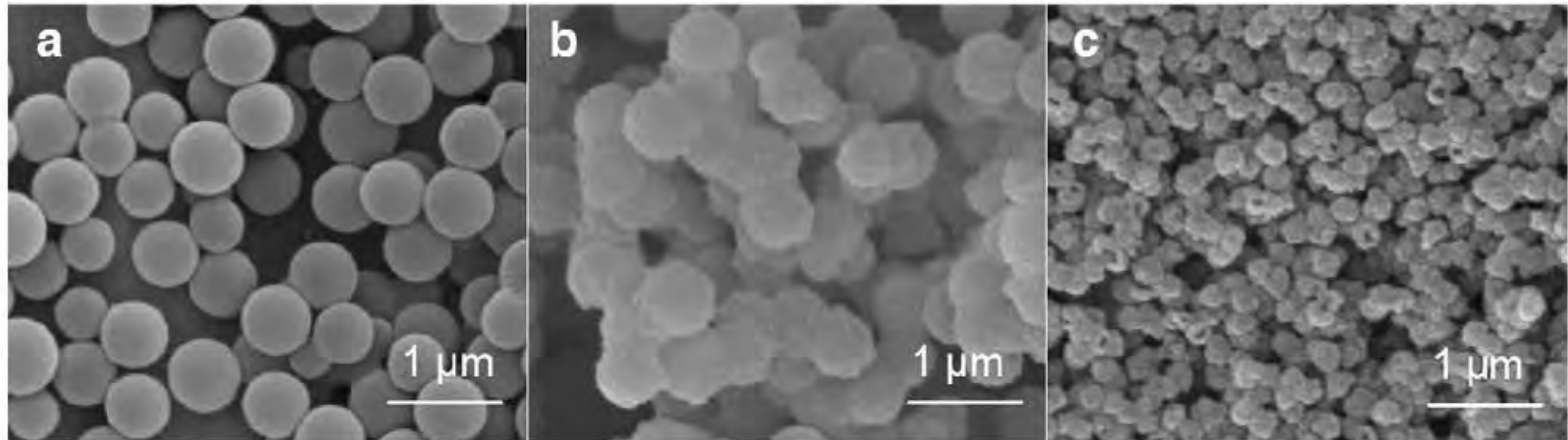
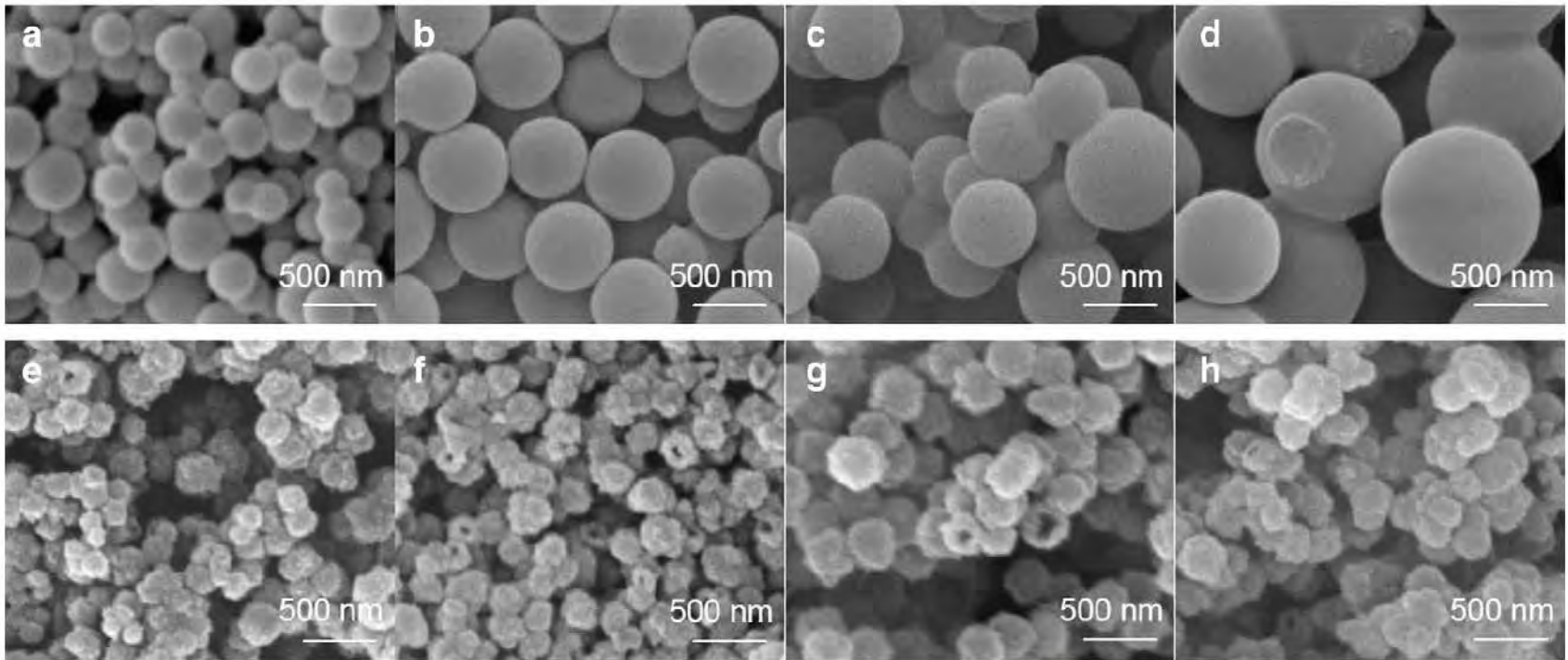


Fig. 2. SEM images of samples obtained after each preparation step (a) CS-G<sub>07</sub>; (b) HS<sub>07</sub>-pre; (c) HS<sub>07</sub>-450.



**Fig. 3.** SEM images of (a–d) carbon sphere templates (CS-G<sub>n</sub>) prepared using different concentrations of glucose solution, and (e–h) TiO<sub>2</sub> hollow spheres (HS<sub>n</sub>-T) obtained after removal of carbon templates by calcination at 450 °C. (a) CS-G<sub>05</sub>; (b) CS-G<sub>07</sub>; (c) CS-G<sub>10</sub>; (d) CS-G<sub>15</sub>; (e) HS<sub>05</sub>-450; (f) HS<sub>07</sub>-450; (g) HS<sub>10</sub>-450; (h) HS<sub>15</sub>-450.

The generation of holes in the TiO<sub>2</sub> shells is caused by the evolution of CO<sub>2</sub> during the removal of the internal carbon spheres reveal the hollow structure of the calcined particles.



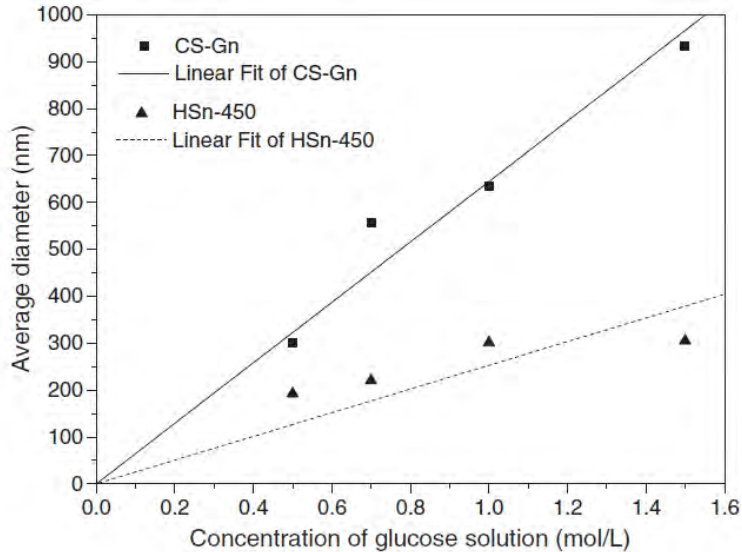
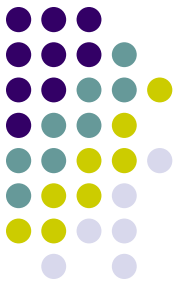


Fig. 4. Average diameter of CS-Gn and HSn-450 spheres vs. concentration of glucose solution.

In addition, graphs of the average diameter of CS-Gn and HSn-450 vs. the concentration of the glucose solution (Fig. 4) were linear. Therefore, the diameter of the carbon sphere template can be easily controlled by adjusting the concentration of the glucose solution, and TiO<sub>2</sub> hollow spheres of different size can be prepared by using different sized carbon spheres as the template.



The thickness of the shell is about 28 nm,  
the diameter of the spheres is 200 nm,

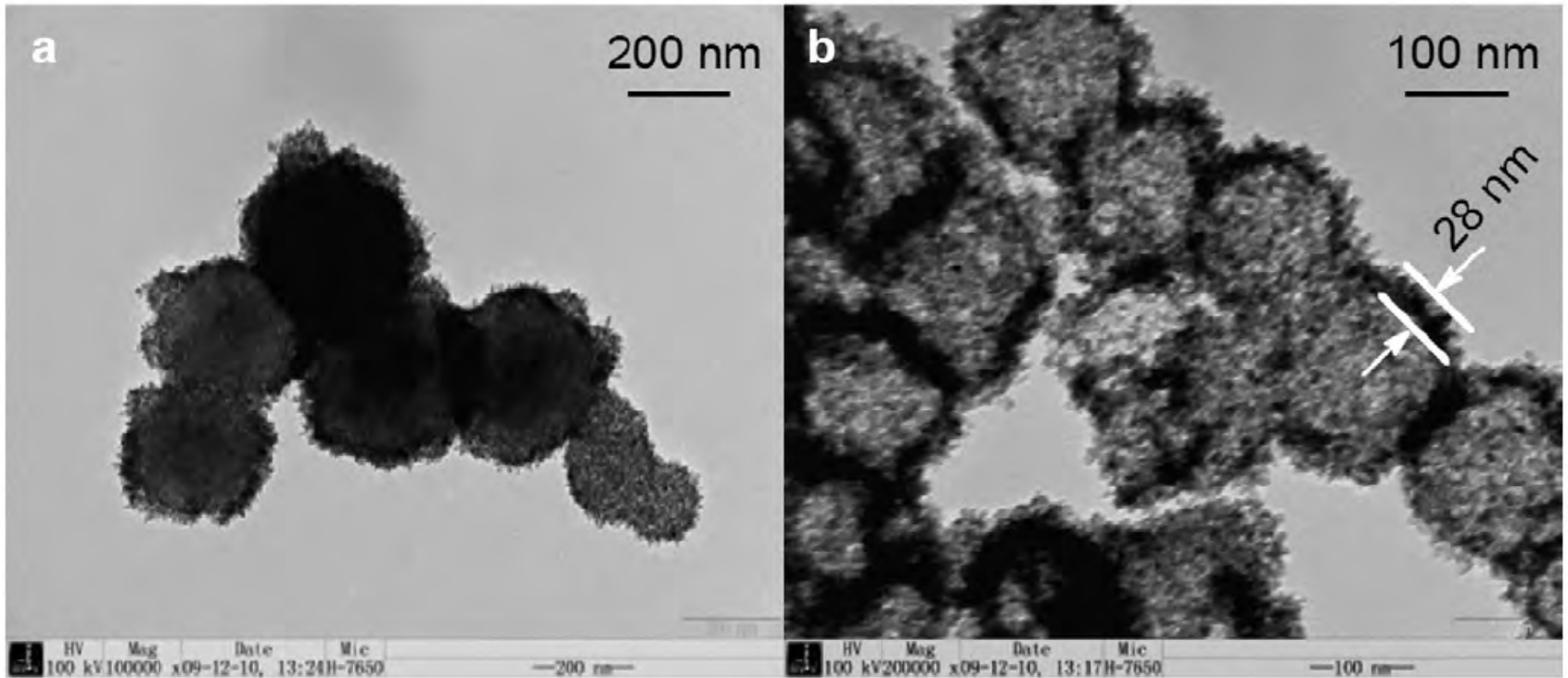


Fig. 5. TEM images of (a) HS<sub>07</sub>-pre and (b) HS<sub>07</sub>-450.

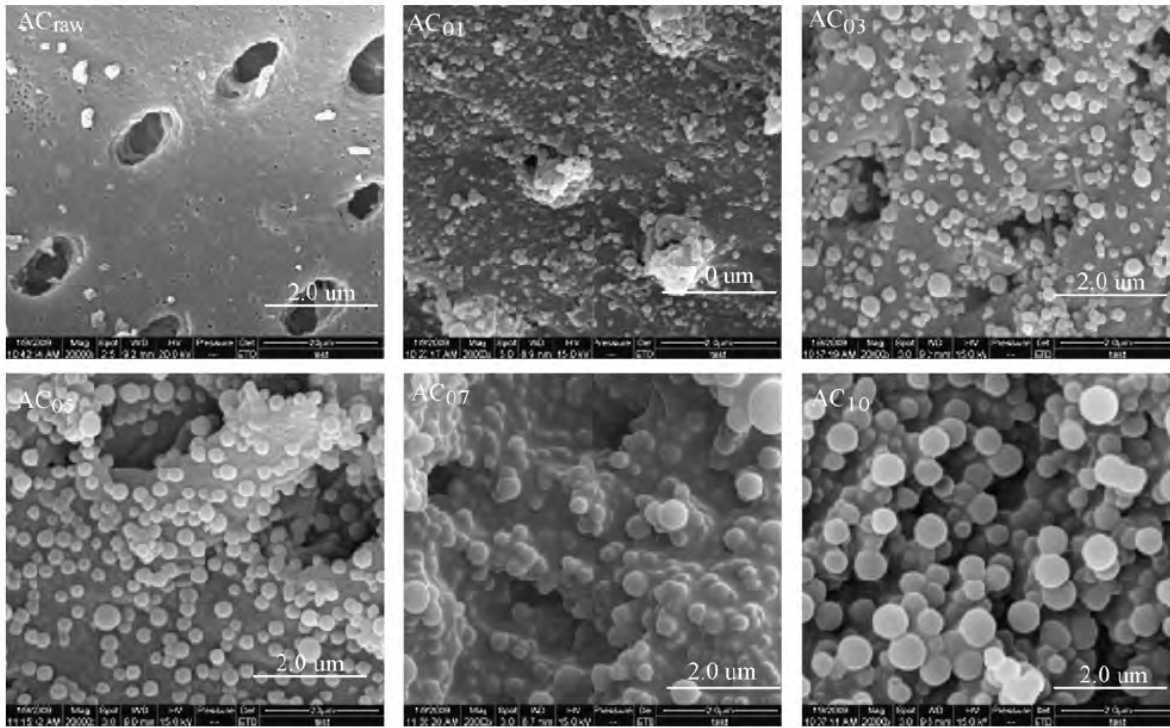
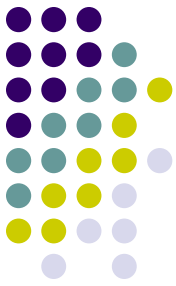


Fig. 1. SEM images of the carbon sphere/AC composites.

When the glucose concentration was  $<0.5 \text{ mol L}^{-1}$ , the AC surface was covered with a monolayer of carbon spheres with sizes in the range 50–200 nm. Increasing the sugar concentration increased the diameter and reduced the size distribution of the carbon spheres. When the glucose concentration was  $0.7 \text{ mol L}^{-1}$ , the AC surface was completely covered with carbon spheres, and a second layer of 300–500 nm diameter spheres was formed. A further increase of the sugar concentration to  $1.0 \text{ mol L}^{-1}$  resulted in a multilayer arrangement of carbon spheres, and the AC surface was covered to the extent that very few of the AC macropores were visible.



**Table 2**

Quantitative XPS results for the presence of surface oxygen in the carbon sphere-AC composites. All values in at%.

Sample	O	C
AC <sub>raw</sub>	10.2	89.80
AC <sub>01</sub>	23.08	76.92
AC <sub>05</sub>	24.62	75.38
AC <sub>10</sub>	30.42	69.58

**Table 3**

Parameters obtained from curve-fitting of the Freundlich and Langmuir equations to the experimental data for the carbon sphere/AC composites.

Adsorbent	Freundlich			Langmuir		
	$k$	$n$	$r^2$	$q_m$	$k$	$r^2$
AC <sub>raw</sub>	0.02807	0.40383	0.9863	0.1660	1.0302	0.9473
AC <sub>01</sub>	0.07547	0.66533	0.9800	0.4834	0.508	0.9581
AC <sub>10</sub>	0.0614	0.61733	0.9717	0.3410	0.671	0.9937

**Table 4**

Adsorption capacity for CrO<sub>4</sub><sup>2-</sup> on the prepared carbon sphere/AC composites per unit mass and per unit surface area.

Sample	CrO <sub>4</sub> <sup>2-</sup> adsorption capacity (mmol g <sup>-1</sup> )	CrO <sub>4</sub> <sup>2-</sup> adsorption capacity (mmol m <sup>-2</sup> )
AC <sub>raw</sub>	0.1236	1.4227 × 10 <sup>-4</sup>
AC <sub>01</sub>	0.4834	1.0961 × 10 <sup>-3</sup>
AC <sub>03</sub>	0.3585	1.0070 × 10 <sup>-2</sup>
AC <sub>05</sub>	0.3462	1.2020 × 10 <sup>-2</sup>
AC <sub>07</sub>	0.2554	1.0641 × 10 <sup>-2</sup>
AC <sub>10</sub>	0.2867	1.3523 × 10 <sup>-2</sup>

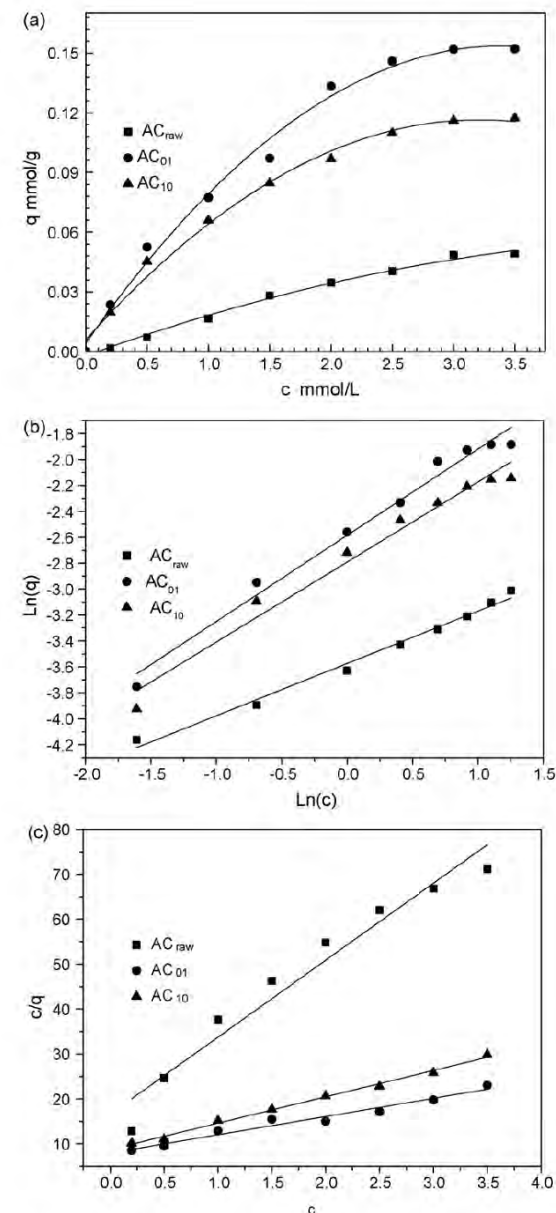
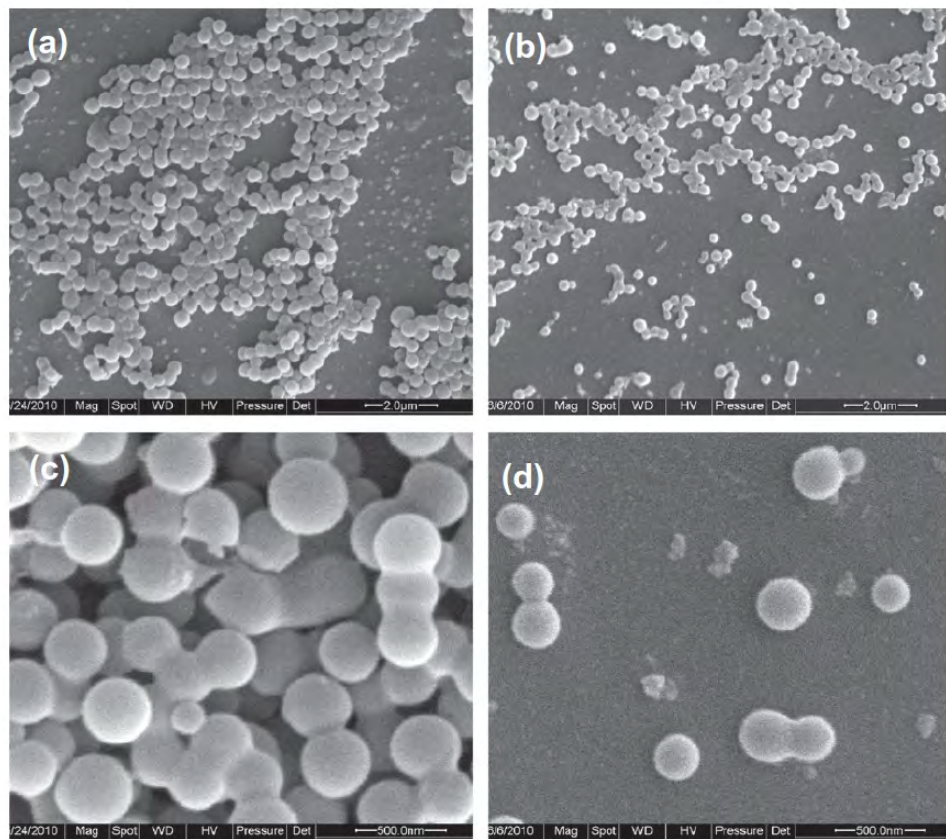
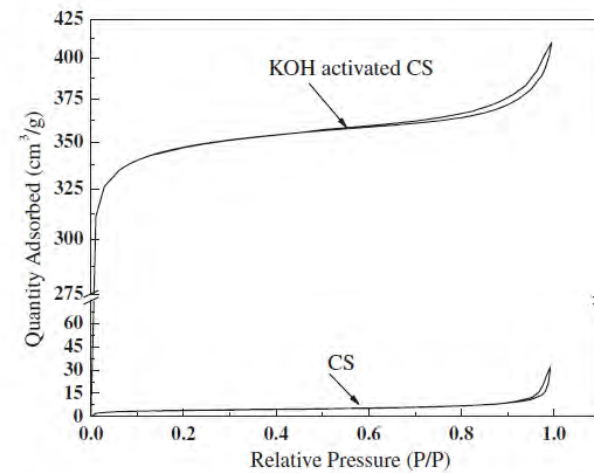


Fig. 7. Adsorption isotherms (a), Freundlich plots (b) and Langmuir plots (c) of CrO<sub>4</sub><sup>2-</sup> on the carbon sphere/AC composites.





**Figure 6.** SEM images of CSs before (a and c, 0.3 mol/L of glucose, prepared at 190 °C for 4 h) and after (b and d) KOH ac

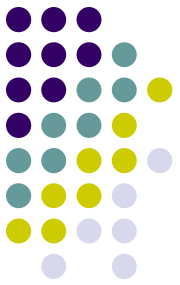


**Figure 7.** Nitrogen adsorption-desorption isotherms of CSs (0.3 mol/L of glucose, prepared at 190 °C for 4 h) before and after KOH activation.

**Table 1**

Textural properties of CSs (0.3 mol/L of glucose, prepared at 190 °C for 4 h) before and after KOH activation

Sample	$S_{\text{BET}}$ ( $\text{m}^2 \text{g}^{-1}$ )	$S_{\text{micro}}$ ( $\text{m}^2 \text{g}^{-1}$ )	$V_t$ ( $\text{cm}^3 \text{g}^{-1}$ )	$V_{\text{micro}}$ ( $\text{cm}^3 \text{g}^{-1}$ )	$V_{\text{meso}}$ ( $\text{cm}^3 \text{g}^{-1}$ )	Ratio <sub>micro</sub> (%)
CS	13.9	1.9	0.03	0.001	0.03	2.9
Activated CS	1283	1013	0.61	0.44	0.18	72



# ACKNOWLEDGEMENT

- Research Fund for the Doctoral Program of Higher Education of China (20100062110003)
- The National Natural Science Foundation of China (31170545)
- The Fundamental Research Funds for the Central Universities (DL11EB01).